ASAR LEVEL 1 GEOLOCATION

David Small[(1)], Detlev Kosmann[(2)], Juergen Holzner[(2)], Hannes Raggam[(3)], Mauro Pirri[(4)], Adrian Schubert[(1)], Urs Kruettli[(1)], Wolfgang Hummelbrunner [(3)], Martina Franke [(3)]

[(1)]Remote Sensing Laboratories, University of Zurich, Winterthurerstr. 190; CH-8057 Zurich, Switzerland, Email:david.small@geo.unizh.ch

[(2)]German Aerospace Centre / DLR, D-82234 Wessling, Germany, Email:Detlev.Kosmann@dlr.de

[(3)]Joanneum Research, Steyrergasse 17, A-8010 Graz, Austria, Email:johann.raggam@joanneum.at

[(4)]Telespazio, Matera Space Centre, C. da Terlecchia, I-75100 Matera, Italy, Email:mauro_pirri@telespazio.it

1 INTRODUCTION

The localisation of ASAR products is vital to the ground segment, as overlays with independent information sources (typically in a map geometry) are only possible when the transformation between radar and map geometry is well calibrated. In this paper we describe calibration and validation steps undertaken to ensure that the transformations from radar to map geometry and back again are as accurate as possible. The ground segment of every new system must validate its geocoding chain to ensure that all parameters are treated consistently and are compatible with the product specifications [2]. Experiences with ERS-1 geopositional accuracy were reported in [5].

Special attention is devoted to the range and azimuth timing, as well as the orbit quality, cartographic and geodetic parameters describing the reference map projections.

ASAR IMS and APS products are in the radar's native slant-range geometry. IMP, APP, IMM, APM, and WSM products are arranged in ground-range geometry. IMG and APG products are ellipsoid-geocoded (no terrain corrections applied), and delivered in map geometry. Each product type requires a slightly different calibration and validation methodology.

The work presented here from DLR was conducted within the *ESA Announcement of Opportunity programme AO762*. Work from the Remote Sensing Laboratories (RSL) and Joanneum Research (Graz) was performed within the ESA-DLR contract "*Contributions of RSL & Graz to the ERS-ENVISAT Ground Segment*".

2 ANALYSIS METHODOLOGY AND TOOLS

In this section we describe the main approaches used for calibrating and validating the ASAR image products. Measurements of accessible features from the image products were compared with map-geometry coordinates read from topographic maps, or with predicted transponder locations based on the orbit and geometry annotations.

In the case of IMG & APG products already in map geometry (typically UTM), coordinates of accessible features were converted to the reference geometry (e.g. Dutch Oblique Stereographic for The Netherlands) and then directly compared. For slant- or ground-range products, a nominal geocoding was conducted to bring the images into the reference geometry, and ground control points were compared directly by juxtaposing map and image measurements.

Being derivative in nature, the geolocation grid (LADS) within the product headers [2] was ignored during the processing described here, in favour of the primary timing information.

2.1 Geocoded Ellipsoid Corrected IMG & APG Product

Ground control points such as bridges, road, and canal intersections were measured both within the ellipsoid-geocoded image and topographic maps. IMG and APG products are typically delivered in a Universal Transverse Mercator (UTM) map projection, necessitating a transformation from that coordinate system into the projection system of the topographic maps used.

We also examined the radiometric performance of the IMG by evaluating the peak and integrated sidelobe ratios (PSLR & ISLR) as well as the 3dB width for transponders in the Netherlands.

2.2 Slant Range IMS Product: Transponders

The locations of the four ESA transponders within the Netherlands as well as their delays were used to predict the position, in range and azimuth coordinates, of their expected appearance within each product. The position of each transponder is first transformed from WGS84 geographic values into global Cartesian coordinates. The position along the orbit t_{az} is then found that satisfies the zero-Doppler condition, via Eqn. (1):

$$f_{D_{ref}} = 0 = \frac{2}{\lambda} \times \frac{(S-P)}{|S-P|} \times (v_p - v_s), \qquad \textbf{(1)}$$

where P is the transponder and S the spacecraft position in Cartesian space, and v_p and v_s are their respective velocities. The condition is solved using the orbital state vectors and timing parameters read from the product header annotations [2]. The "expected" range R_t of the transponder in the image is then calculated via Eqn. (2):

$$R_t = |S-P| + t_{Delay} \times \frac{c}{2}, \qquad \textbf{(2)}$$

where t_{Delay} is the transponder's delay, and c is the speed of light. The SLC image coordinates are then easily derived from t_{az} and R_t.

This "predicted" position was then compared with the actual measured location of the transponder within each image. Since the transponders are distributed across the Netherlands, not all appear within the bounds of every scene. For the visible transponders, the mean azimuth and range differences were calculated within each scene.

2.3 Radar Geometry IMS & IMP Products: Map-based Ground Control Points

The geometric localisation of the same slant range IMS products was also evaluated using conventional ground control points – for example, bridges, road and canal intersections. The IMS products were first "terrain" geocoded using the best available digital elevation model and orbit data, using the localisation algorithm described in Section 2.2. Ground control points were then measured from the geocoded terrain corrected (GTC) image as well as from topographic maps. Mean and standard deviation of the difference was derived for each scene.

3 DATA SET OVERVIEW

3.1 Flevoland, The Netherlands

The datasets and auxiliary data available for our tests covering Flevoland (The Netherlands) are listed in **Table 1**. A variety of orbit qualities, ascending / descending geometries were available. The early products were range compressed using a chirp replica; the latter products were all processed using the nominal range chirp.

Dutch topographic maps at scales of 1:25000 and 1:50000 were available, as well as a DEM (derived from GTOPO30) in the same Dutch oblique stereographic map projection, sampled at a spacing of 12.5 metres.

Orbit	*Orbit Quality*	*Asc / Desc*	*Product Type*	*Beam*	*Range Chirp Type*
2130	Predicted	A	IMG, IMP	IS3	Replica
2166	Predicted	D	IMS	IS3	Replica
670	Restituted	A	IMS	IS4	Replica
706	Restituted	D	IMS	IS2	Replica
670	Predicted	A	IMS	IS4	Nominal
706	Predicted	D	IMS	IS2	Nominal
1894	Precise	D	IMS	IS4	Nominal
2209	Precise	D	IMS	IS2	Nominal

Table 1 - ENVISAT ASAR Datasets

4 IMG – GEOCODED ELLIPSOID CORRECTED ESA PRODUCTS

A single IMG product covering Flevoland (The Netherlands) was investigated for geometric accuracy (orbit 2130). Points were measured in the UTM projection IMG product, and transformed into the Dutch oblique stereographic coordinate system. In comparison to map measurements, the following offset statistics were derived: -262.3±71.9m in Easting, and 33.9±53.6m in Northing. Later investigations showed that a large part of this error was due to a faulty chirp replica having been used during range compression. We have not yet repeated these tests on an IMG product processed with a nominal chirp, but, based on experiences with IMS products (discussed below), expect significant improvement. Due to the nature of ellipsoid geocoding, larger errors would result if such a test were done in an area with significantly more terrain variation than the relatively flat Dutch landscape. **Figure 1** shows the IMG product (orbit 2130) investigated by Telespazio. An image overview is displayed in (a), with close-ups of the two visible transponders, Edam and Swifterbant, in (b). Range and azimuth profiles for the two transponders are shown in (c).

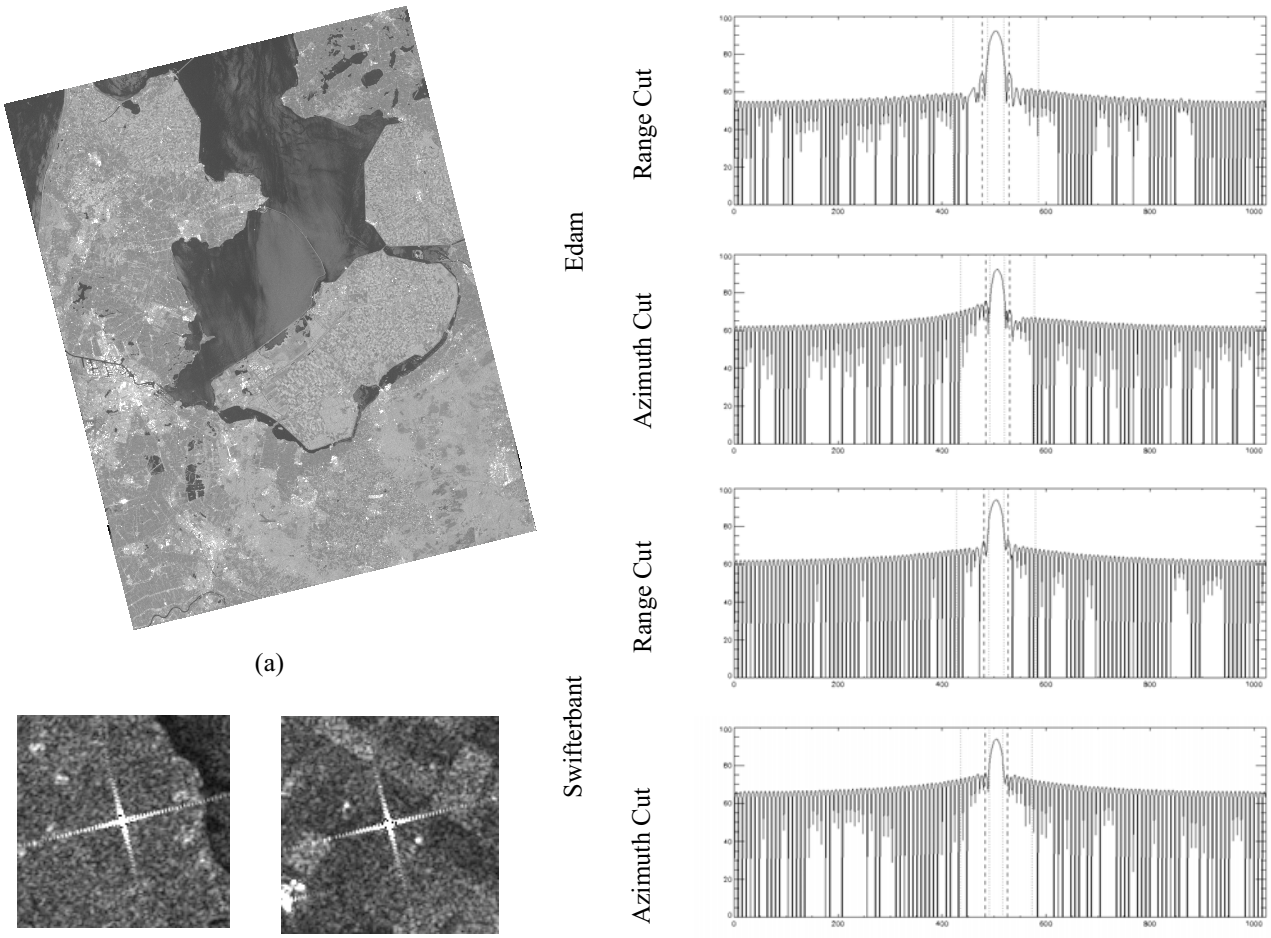

Figure 1: Flevoland IMG Product, Orbit 2130 IS3 VV: (a) IMG image overview, (b) Transponder Close-ups, (c) Range and azimuth cuts illustrating PSLR, ISLR, 3dB width

	Parameter	***Value***		***Parameter***	***Value***	***Limit***
Edam	ISLR	-9.44dB	*Swifterbant*	ISLR	-7.77dB	< **-7dB** (12+5)
	PSLR	-16.57dB		PSLR	-17.96dB	< **-15dB** (-20+5)
	3dB Width	25.9 x 22.3m		3dB Width	23.9 x 21.7m	< **33m**

Table 2 - IMG Transponders - Radiometric Performance

The ISLR, PSLR, and 3dB width values measured from the IMG product are shown to be within acceptable limits in **Table 2**. Bilinear resampling was used during the standard IMG ellipsoid geocoding – the ISLR value might be improved through the use of a larger resampling kernel.

5 IMS – SINGLE LOOK COMPLEX ESA PRODUCTS

5.1 Transponder Locations: Predicted vs. Measured

The location of each of the four ESA transponders was predicted based on their location, delay, and orbit annotations, and compared with the actual location of the transponder within the image. The two locations are juxtaposed in **Figure 2** for the orbits 670, 706, 1894, and 2209. The predicted location is shown with the blue cross-hairs; the actual transponder location is apparent, if visible. The transponder Zwolle appears not to have responded in scenes 706 and 2209, and was outside the scene boundaries of 670 and 1894. The Aalsmeer transponder was outside the scene boundary of orbit 2209.

Results for orbits 670 and 706 should be partially discounted due to the poorer quality of their predicted orbits [1]. The 1894 and 2209 products were processed with precise orbits.

A quantitative comparison of predicted and measured transponder locations for the scenes processed with a nominal chirp is provided in **Table 3**. The relatively large azimuth biases in the scenes from orbits 670 and 706 are probably due to the poor quality of the predicted orbits used. Given more data sets, the range bias may be useful to validate the ASAR's sampling window start time bias.

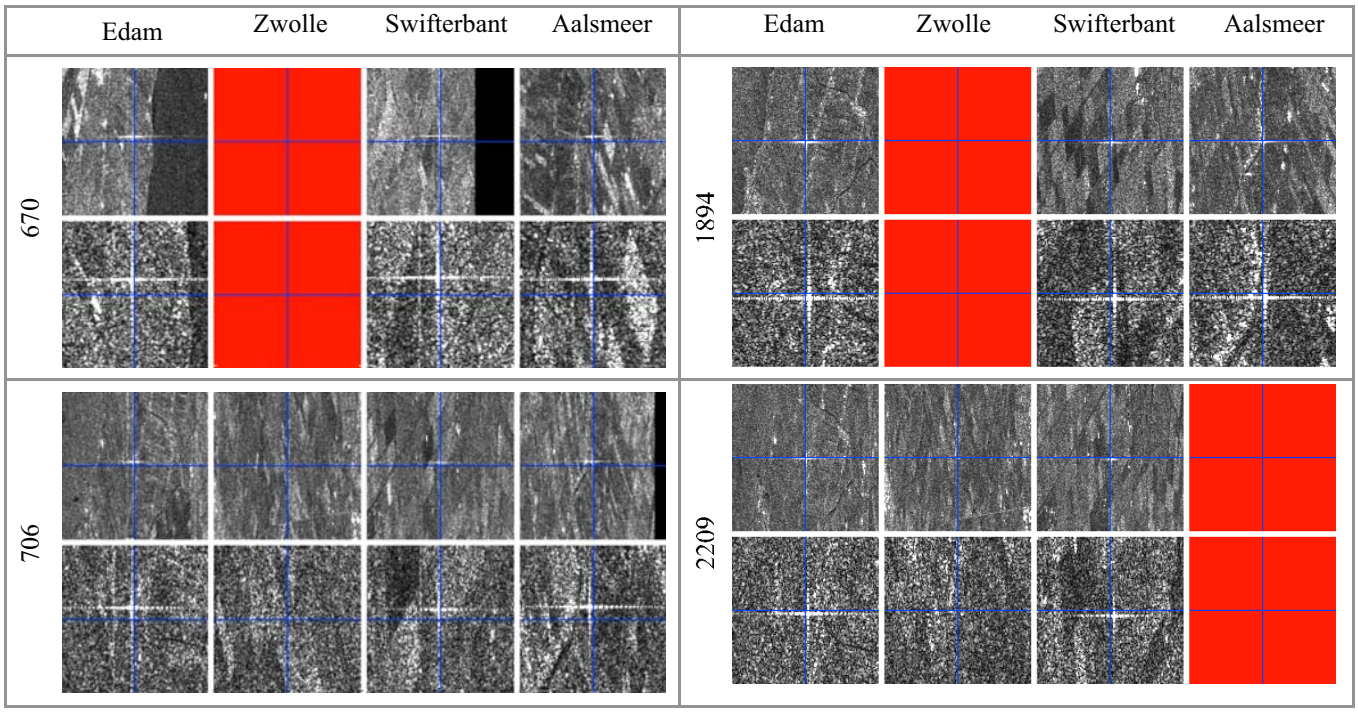

Figure 2 - ESA Flevoland transponders for orbits 670, 706, 1894, 2209 – Predicted (blue cross) vs. image coordinates. Top row: 3x3 average, Bottom row: native SLC resolution. Red indicates transponder was outside the scene.

5.2 Geocoding Validation

Detected and multi-looked versions of the input IMS images are shown in **Figure 3**, together with "terrain"-geocoded counterparts, overlaid on the GTOPO30 model used. Ground control points were measured within the terrain-corrected products to validate the geocoding process. It should be emphasized that no points were used to refine the imaging geometry – all geolocation was performed using the nominal imaging parameters retrieved from the product headers.

Orbit	*Azimuth difference [SLC samples]*	*Range difference [SLC samples]*
670	13.9	1.8
706	10.4	2.2
1894	-4.3	-3.0
2209	-3.9	-3.2

Table 3 - Differences between predicted and measured transponder locations

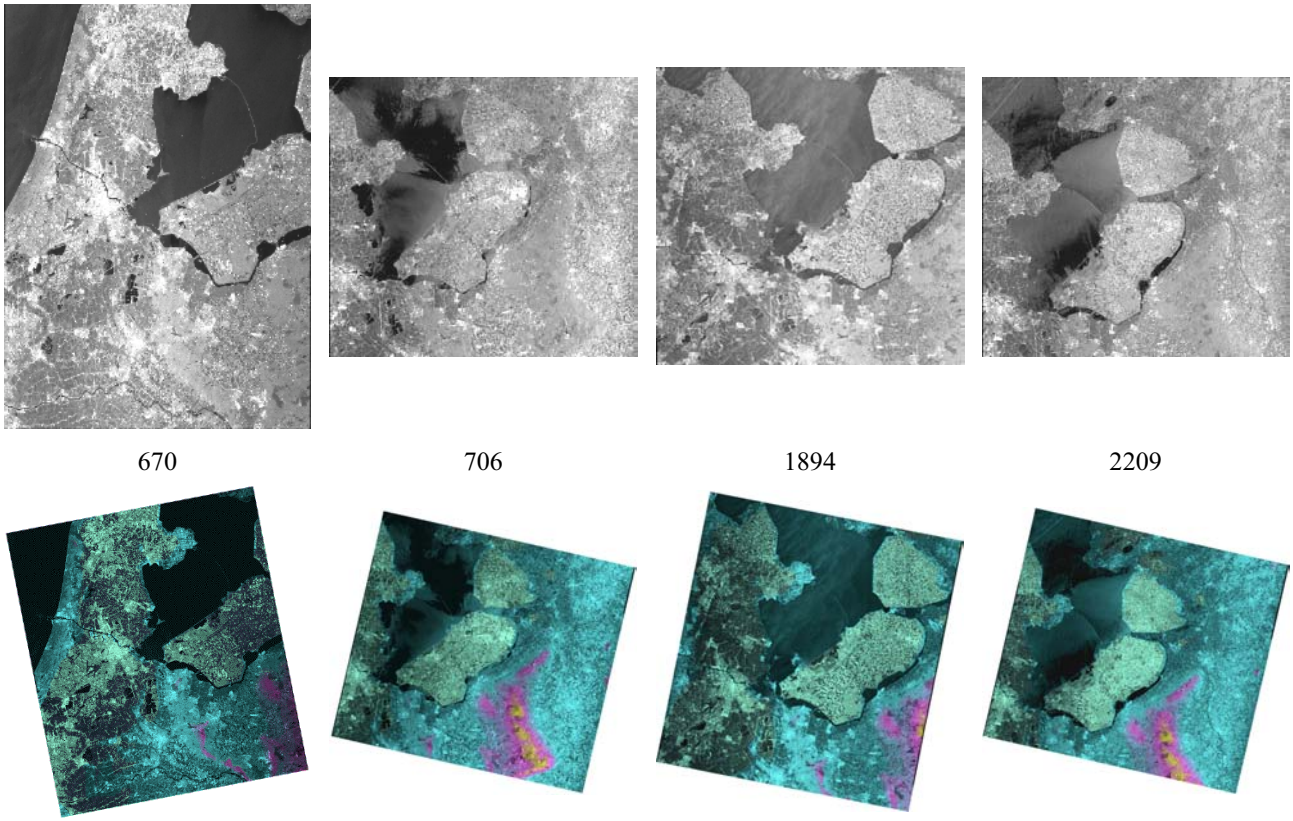

Figure 3 - Top row: IMS nominal chirp input images (range, azimuth geometry); Bottom row: terrain-geocoded images (Dutch oblique stereographic map projection) – GTOPO30 height 120m colour cycle underlaid

The mean and standard deviations of the differences between the GTC and map coordinates of identifiable features such as bridges, road, and canal intersections are listed in **Table 4**. These describe the estimated dislocation of the GTC in map geometry. The results are based on 13-20 GCP measurements per scene. Note the large improvement in accuracy when range compression is performed using the nominal chirp, rather than the replica [3].

Considering only those scenes range-compressed with the nominal chirp, geolocation accuracy is generally quite acceptable, especially considering that all geocoding was performed with a-priori non-refined imaging parameters. Differences are higher for the scene from orbit 706. This may be due to the fact that it is the only available nominal-chirp processed scene where the sign of the range and azimuth biases together with the ascending/descending geometry cause the range and azimuth errors to be additive during geocoding rather than counteract each other. The differences for the other (nominal chirp) scenes are lower than would be expected from the transponder results, probably due to the opposite effect.

Dataset	*Chirp*	*Easting Difference*	*Northing Difference*
IMP 2130	Replica	-126.6 ± 19.3 m	-19.3 ± 13.7 m
IMS 2166	Replica	169.5 ± 11.9 m	-40.5 ± 10.1 m
IMS 670	Replica	-121.6 ± 17.6 m	-58.3 ± 13.5 m
IMS 706	Replica	135.6 ± 12.7 m	-21.1 ± 10.8 m
IMS 670	Nominal	8.4 ± 15.6 m	-28.0 ± 7.5 m
IMS 706	Nominal	75.4 ± 11.3 m	42.3 ± 11.0 m
IMS 1894	Nominal	-7.9 ± 18.2 m	-3.4 ± 10.7 m
IMS 2209	Nominal	-24.9 ± 14.5 m	3.5 ± 11.8 m

Table 4 - Geolocation validation in Dutch oblique stereographic projection – mean and standard deviation of difference between GTC coordinates and map measurements

Dataset	*Beam*	*Requirement*	*Measurement*
IMP 2130	IS3	**79.6** km	82.9 km
IMS 2166	IS3	**79.6** km	83.3 km
IMS 670	IS4	**85** km	87.7 km
IMS 706	IS2	**100** km	106 km
IMS 1894	IS4	**85** km	87.8 km
IMS 2209	IS2	**100** km	105.5 km

Table 5 - Swath width validation – all scenes examined pass test

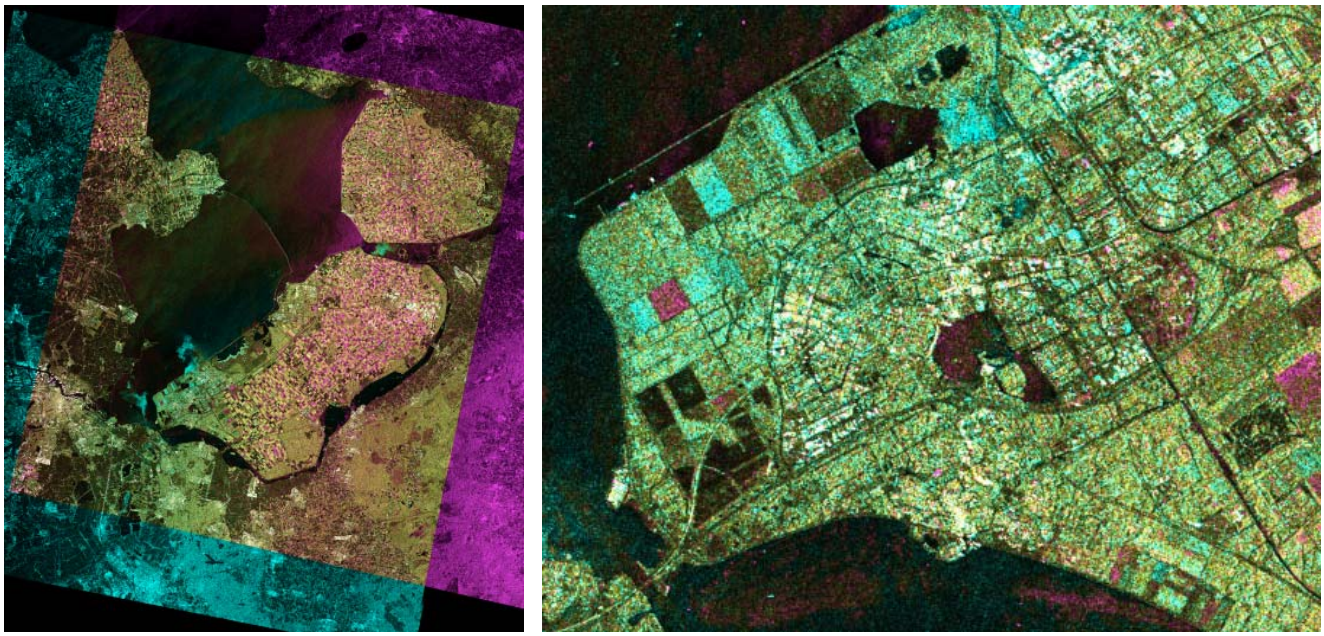

(a) Overlap Region – Flevoland (NL)

(b) Close-up of *Almere-Stad* Region

Figure 4 - Overlay of unrefined (nominal geometry) terrain-geocoded detected IMS products from orbits 1894 & 2209

During terrain geocoding, the swath width was measured for each product and compared with the requirement for the beam in question. Results are listed in **Table 5**: all products checked so far have passed the minimum swath width test.

Another test of geolocation accuracy is inspection of an overlay of two geocoded products for signs of deviations from ideal coincidence of identifiable high contrast features. An RGB (R=2209/G=1894/B=|1894-2209|) overlay of the GTC products from the orbits 1894 (IS4) and 2209 (IS2) is shown in **Figure 4**. Shifts are not readily apparent, even when inspected at the full GTC sampling interval – note, for example, the excellent correspondence of the pier at the top left of **Figure 4**(b), and the street network.

5.3 Medium Resolution Products

Geolocation requirements are less stringent for medium resolution products. However, the products have unique properties that must be accounted for to ensure accurate results. For example, orbit state vectors are often not distributed regularly in time, as shown in **Figure 5**(a). Orbit input software must account for the irregular spacing. In addition, medium resolution products are also often annotated with multiple slant/ground range polynomials that must be accounted for in any map/image geolocation problem.

Ground control points were measured in IMM and IMP products, as shown in **Figure 5**(b), with large sporadic errors of up to 15 km being reported by Joanneum Research for scenes covering Garmisch-Partenkirchen in southern Germany and Austria.

Significant shifts were measured in a wide swath mode image covering southern Germany, Switzerland, western Austria, and northern Italy nominally terrain-geocoded using a GLOBE DEM: see **Figure 5**(c). Validation becomes more difficult in such large scenes, as multiple map projections and geodetic reference systems introduce a further error source. Accurate datum shift parameters for all reference systems gain even more importance in such situations.

WSM and IMM products covering mountainous regions could be compared to image simulations [6] based on DEM's in a near-automatic validation of the geometry parameters, effectively using the topography as a source of thousands of GCP's.

Issues unique to medium resolution products gain urgency as the IMS geolocation becomes increasingly satisfactory.

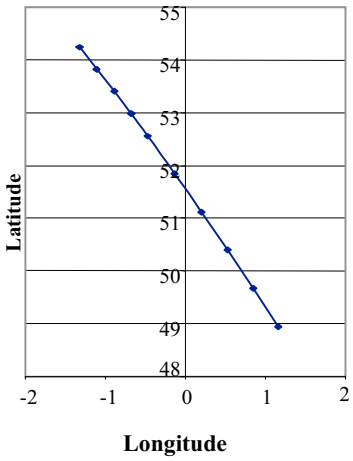

(a) Irregularly spaced state vectors

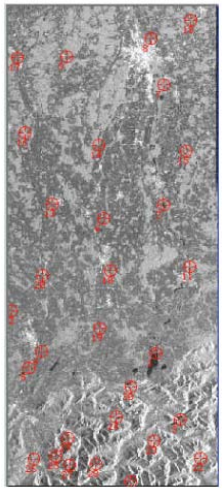

(b) GCP's in Bavaria & Austria

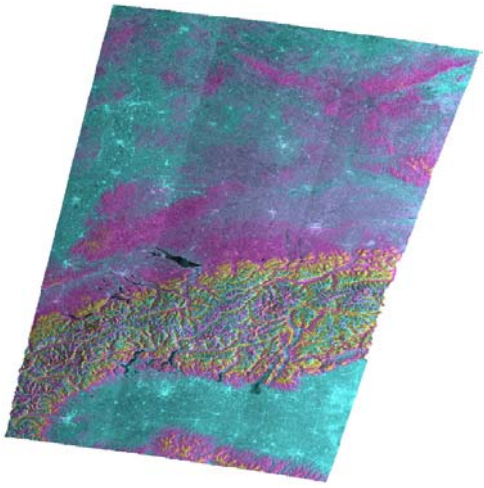

(c) Wide Swath Mode – Alpine Central Europe (Southern Germany, Switzerland, Austria, Northern Italy) Terrain-geocoded, colour cycle 2000m

Figure 5 - Medium Resolution Products – irregularly spaced state vectors, IMM, WSM

6 SUMMARY, CONCLUSIONS, AND OUTLOOK

Localisation results were significantly improved when a nominal chirp was used rather than a chirp replica during range compression. Achieved localisation accuracies were similar for predicted and restituted orbits in the two pairs of scenes tested. Localisation accuracy as measured by both predicted vs. measured transponder locations and GTC validation improved when precise orbits were used.

More scenes, beams, and modes will have to be processed with the nominal chirp for definitive validation. Adjustments to the nominal sampling window start time (SWST) may then be considered. Validation of medium resolution geolocation will gain in importance as IMS geocoding becomes operational.

Inter-comparisons with results from diverse groups will continue in ongoing efforts to converge on a consensus validation of ASAR geolocation accuracy.

7 REFERENCES

[1] ASAR Cal/Val Team, *ASAR Cal/Val Implementation Plan*, Issue 1.0, March 2002.

[2] ENVISAT Payload Data Segment, *ENVISAT Products Specification - Volume 8: ASAR Products Specifications*, Jan. 2002.

[3] J. Closa, *Processor Verification*, ENVISAT Calibration Review, ESTEC, Noordwijk, The Netherlands, Sept. 2002.

[4] D. Kosmann, J. Holzner, W. Hummelbrunner, D. Small, *Geometric Accuracy of ASAR Products – Calibration Phase*, Proc. EUSAR 2002, Cologne, Germany, June 4-6, 2002, pp. 471-474.

[5] A. Roth, T. Hügel, D. Kosmann, M. Matschke, G. Schreier, *Experiences with ERS-1 SAR geo-positional accuracy*, Proc. IGARSS'93, Tokyo, Japan, pp. 1450-1452.

[6] D. Small, S. Biegger, D. Nüesch, *Automated tiepoint retrieval through heteromorphic image simulation for spaceborne SAR sensors*, Proc. of ERS-ENVISAT Symposium, ESA Publication SP-461, Gothenburg, Sweden, Oct. 16-20, 2000.

[7] M. Zink, *ASAR Calibration Review Introduction*, ENVISAT Calibration Review, ESTEC, Noordwijk, The Netherlands, Sept. 2002.